Journal of the European Ceramic Society 19 (1999) 993–997

PII: S0955-2219(98)00360-4
0955-2219/99/$ - see front matter

Fabrication of Piezoelectric Particle-dispersed Ceramic Nanocomposite

Hae Jin Hwang,[a]* Toru Nagai,[b] Mutsuo Sando,[a] Motohiro Toriyama[a] and Koichi Niihara[c]

[a]National Industrial Research Institute of Nagoya, Nagoya 462-8510, Japan
[b]Nippon Steel Corporation, Kawasaki 211-0035, Japan
[c]The Institute of Scientific and Industrial Research, Osaka University, Osaka 567-0047, Japan

Abstract

The goal of this study is to fabricate perovskite type ferroelectric particles-dispersed ceramic nanocomposites though conventional hot-pressing or pulse electric current sintering (PECS). This type of nanocomposite is expected to show ferroelectricity or piezoelectricity with retaining mechanical properties. Magnesia (MgO) and barium titanate ($BaTiO_3$) were selected as a matrix and secondary phase dispersoid. From X-ray diffraction analysis, the $BaTiO_3$ was the phase compatible with the MgO matrix, and there were no reaction phases between the matrix and $BaTiO_3$. It was found that the $BaTiO_3$ enhanced the sinterability of the MgO ceramics. Relative density of pure MgO was lower than 80%, while dense MgO/10 vol% $BaTiO_3$ nanocomposites could be successfully prepared by sintering at 1200°C for 10 min through PECS method. Fine $BaTiO_3$ particles were homogeneously dispersed within the MgO matrix grain as well as at grain boundaries. Sintering behavior and microstructure development of the MgO/$BaTiO_3$ nanocomposites were discussed in terms of $BaTiO_3$ content and sintering temperatures. © *1999 Elsevier Science Limited. All rights reserved*

Keywords: hot pressing, nanocomposites, mechanical properties, MgO, perovskite.

1 Introduction

Since *ceramic nanocomposites*, materials reinforced by secondary dispersoids of a few tens to a few hundreds of nano meter in size (nano particle) were proposed in the field of engineering ceramics by Niihara and his colleagues, silicon carbide- or silicon nitride-dispersed nanocomposites, e.g. alumina/silicon carbide, alumina/silicon nitride and silicon nitride/silicon carbide were fabricated.[1,2,3] In these nanocomposites, nanometer sized silicon carbide and silicon nitride were successfully distributed in alumina or silicon nitride matrix grains or grain boundaries in the range of 5 to 20 vol%, and significant improvements in mechanical properties, such as fracture strength, hardness and fracture toughness have been reported. High temperature mechanical properties were also improved.[4]

The advantages to be derived by introducing *softer* secondary dispersoids than the matrix, like boron nitride or metallic particles are also of great concern because such particles would render the nanocomposites into the possibilities of new properties or functions.[5,6] In alumina/nickel nanocomposite, for example, inverse magnetostriction effect of metallic nickel particles can give the composite a remote sensing capability of the mechanical stress that is acting on the composites[7] Moreover, the alumina/nickel nanocomposite showed excellent fracture strength, and it means the possibility of introducing into engineering ceramics new functions with improving mechanical properties.

From the viewpoint of mechanical properties, ferroelectricity or piezoelectricity shows an interesting property. By utilizing a electromotive force of the ferroelectric material, we are able to detect a crack propagation.[8] When the ferroelectric materials are subjected to an electric field, additional internal stresses are induced; since the internal stresses are anisotropic, thus they can increase or decrease fracture toughness, depending on the poling direction.[9] In this regard, ferroelectric particle-dispersed ceramic nanocomposite is expected to exhibit such intelligent functions that are capable of predicting the fracture, controlling the crack

*To whom correspondence should be addressed. Fax: +81-52-916-2802; e-mail: hwang15@nirn.go.jp

propagation and so on. The goal of this study is to fabricate the ceramic nanocomposite that contains perovskite type ferroelectric particles so as to introduce into the nanocomposite ferroelectricity or piezoelectricity. Recently, the authors reported about the fabrication processes and microstructure of ceramic nanocomposite with a perovskite-type ferroelectric dispersoid.[10] It was found that $BaTiO_3$ was the phase compatible with MgO matrix and the $BaTiO_3$ particles were ferroelectric: tetragonal phase. However, some problems still remain unsolved. These include: (1) a loss of oxygen from the perovskite structure during hot-pressing in a reducing atmosphere results in reduced-type $BaTiO_{2.977}$ and (2) a decrease in tetragonality due to a Mg^{2+} substitution for Ti^{4+}. These problems lead to deteriorate the ferroelectricity or piezoelectricity of the nanocomposite.

Pulse electric current sintering (PECS) is one of the solid consolidation process similar to hot-pressing. It is believed that microscopic spark plasma between particles due to the applied pulse voltage enables us to sinter ceramic materials for shorter time and at lower temperature. In addition, self-exothermic effect by the electric discharge between particles at early stage of on-off direct current (d.c.) pulse application can accelerate the sintering. Recent reports indicate the advantages of the PECS technique.[11,12] In this study, the PECS technique was employed to control the reaction between the matrix and second dispersoid. MgO/$BaTiO_3$ nanocomposites were fabricated and sintering behavior and microstructure development of the nanocomposites were investigated in terms of $BaTiO_3$ content and sintering temperature.

2 Experimental Procedures

Barium titanate ($BaTiO_3$) particles-dispersed MgO nanocomposites were prepared by pulse electric current sintering (PECS) technique or conventional hop-pressing. The starting materials for the matrix and dispersoids were commercially available MgO powder (1000A, Ube Industries, Yamaguchi, Japan) and $BaTiO_3$ (BT-03, Sakai Chemical Industry Co. Ltd., Osaka, Japan) powder. Ba/Ti atomic ratio of the $BaTiO_3$ powder was 0·999. The crystal phase of the $BaTiO_3$ was tetragonal. The particle size of the MgO and $BaTiO_3$ powders was 0·1 and 0·3 μm, respectively. MgO and appropriate quantities of $BaTiO_3$ (5, 10, 20, 40, 60, 80 vol%) were wet-milled in a polyethylene container using n-butyl alcohol and ZrO_2 balls for 16 h. Mixed slurries were dried with a rotary evaporator. The dried powder mixtures were sieved through a 320 μm mesh screen and calcined at 800°C for 30 min in air atmosphere. The mixed powders were packed into a carbon die and sintered using PECS system (SPS 3·20 MK-IV, Sumitomo Coal Mining Co. Ltd., Japan) and HP (hot-pressing) system (Fujidenpa Kogyo Co. Ltd., Japan). The samples were heated to prescribed temperatures at heating speeds of 100 and 20°C/min for PECS and HP sintering, respectively. After the duration, the pressure (30 MPa) was relaxed and the specimens were cooled in the furnace. The temperature of the graphite die was measured with a pyrometer. Sintering conditions were 1200 to 1300°C for 5 min (PECS) and 1350°C for 1 h (HP). Sintered bodies were cut and ground using 400- and 800-grit resin-bond diamond wheels. For mechanical property test and microstructure observation, the samples were polished with 9, 3 and 0·5 μm diamond pastes. Monolithic MgO and $BaTiO_3$ were also prepared by the same procedure.

For a phase characterization, X-ray diffraction patterns were obtained on X-ray powder diffractometry (RU-200B, Rigaku Co. Ltd., Japan). The diffraction pattern was taken using Ni-filtered CuK_α radiation. Bulk density was determined via the Archimedes method in water. The grain size of the MgO matrix was estimated from micrographs taken from scanning electron microscope (SEM, JEOL JSM-6320FK), using a linear intercept method. Fracture strength was measured on the bar-shaped specimens (3 × 4 × 40 mm in dimension) by a three-point bending method (MTS808, MTS Systems Corp. MN, USA). A cross-head speed was 0·5 mm min^{-1}.

3 Results and Discussion

Figure 1 shows the X-ray diffraction profiles of MgO/10 vol% $BaTiO_3$ nanocomposites as-hot-pressed at 1350°C for 1 h (a), annealed at 1300°C for 8 h (b) and as-PECSed at 1300°C for 10 min. All of the peaks for the hot-pressed MgO/$BaTiO_3$ nanocomposite [Fig. 1(a)] were assigned to MgO and $BaTiO_3$. Some minor peaks indicated by h in Fig. 1 were found to be hexagonal $BaTiO_3$, $BaTiO_{2.977}$ which is a reduced phase of $BaTiO_3$. It seems that the appearance of the $BaTiO_{2.977}$ is due to the reduced sintering atmosphere produced by graphite die of the hot-pressing. The subsequent annealing process at 1300°C for 8 h needed to oxidize the reduced form of $BaTiO_3$. On the other hand, the MgO/$BaTiO_3$ nanocomposite prepared by PECS technique consisted of MgO and $BaTiO_3$ phases, and there were no $BaTiO_{2.977}$, and also no unwanted reaction phases between the MgO matrix and $BaTiO_3$. Lower temperature and shorter time of the sintering process relative to the hot-pressing,

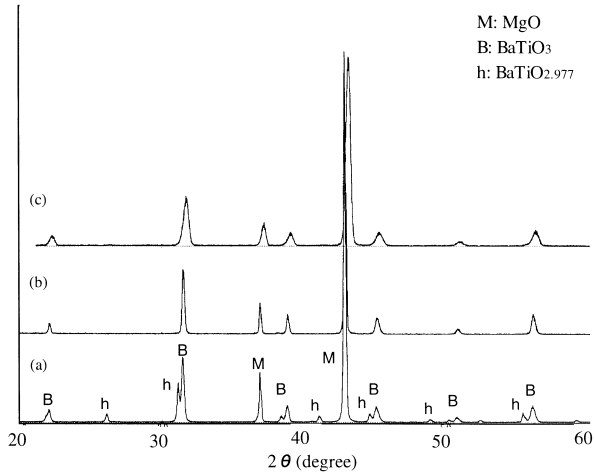

Fig. 1. X-ray diffraction profiles of MgO/10 vol% $BaTiO_3$ nanocomposites as-hot-pressed at 1350°C for 1 h (a), annealed at 1300°C for 8 h (b) and as-PECSed at 1300°C for 10 min (c).

which is the advantage of the PECS technique results in the observed phenomenon. The intensities of $BaTiO_3$ peaks increased with increasing $BaTiO_3$ content, indicating that $BaTiO_3$ is the phase compatible with the MgO matrix in the MgO/$BaTiO_3$ nanocomposites.

SEM photographs for the fracture surfaces of the monolithic MgO and MgO/$BaTiO_3$ nanocomposites PECSed at 1300°C for 10 min are shown in Figs 2 and 3. Fracture mode was found to be predominantly intergranular, and transgranular fracture was also observed for both the monolithic MgO and MgO/$BaTiO_3$ nanocomposites. Figures 2 and 3 indicate that the grain size of the MgO matrix drops significantly with an addition of $BaTiO_3$ particles; the grain size of the monolithic MgO is approximately estimated to be 10 μm, while that of the $BaTiO_3$/20 vol% $BaTiO_3$ nanocomposites is less than 1 μm. During the sintering process, it seems that the $BaTiO_3$ particles which are dispersed in the MgO matrix, control grain boundary movement and limit the grain growth of the MgO matrix.

The white, relative to the MgO matrix and spherical phases in Fig. 2(b) and Fig. 3(a) and (b) are $BaTiO_3$ particles. The $BaTiO_3$ particles were homogeneously dispersed within the MgO matrix grains as well as at grain boundaries. As the $BaTiO_3$ content increased from 5 to 20 vol%, the particle size of the developing $BaTiO_3$ slightly increased, and the ratio of intergranular to intragranular $BaTiO_3$ particles also increased. When the sintering temperature is raised from 1200°C to 1300°C, the particle size of the $BaTiO_3$ is also increased. This means that a part of the $BaTiO_3$ particles, which were initially located between the MgO matrix move along with the grain boundary, gradually becoming concentrated at boundary intersections and coalescing into larger particles as grain growth proceeds.

Relative densities of the various MgO/$BaTiO_3$ nanocomposites sintered by PECS technique are presented in Fig. 4. For the comparison, the relative density of MgO/10 vol% $BaTiO_3$ nanocomposite sintered at 1350°C by hot-pressing was also indicated in Fig. 4. The relative densities of the PECSed composites were higher than those of the hot-pressed ones. It means that the densification was enhanced in the MgO/$BaTiO_3$ nanocomposites by the PECS technique. For example, in the case of the hot-pressed MgO/10 vol% $BaTiO_3$ nanocomposite the relative density was approximately 98%, however, the same relative density could be achieved after sintering the nanocomposite at 1200°C for 10 min by PECS technique. Therefore, it can be inferred that the PECS technique is effective on lowering the sintering temperature of the MgO/$BaTiO_3$ nanocomposites. How the PECS can enhance the sinterability of the MgO/$BaTiO_3$ nanocomposites is not established now. Cleaning

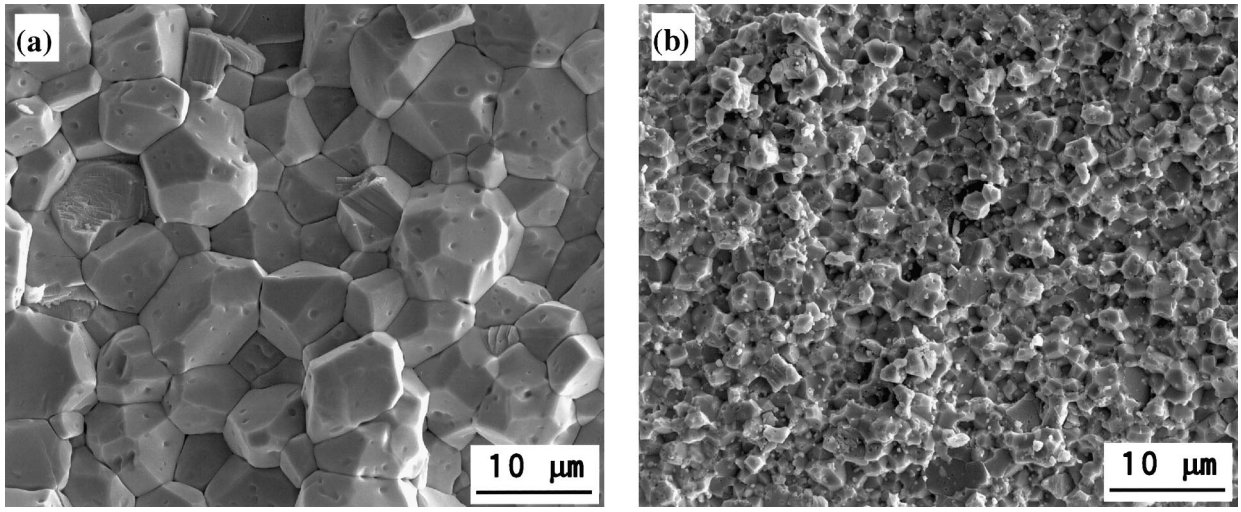

Fig. 2. SEM photographs for the fracture surfaces of the monolithic MgO (a) and Mg0/5 vol% $BaTiO_3$ nanocomposites (b) PECSed at 1300°C for 10 min.

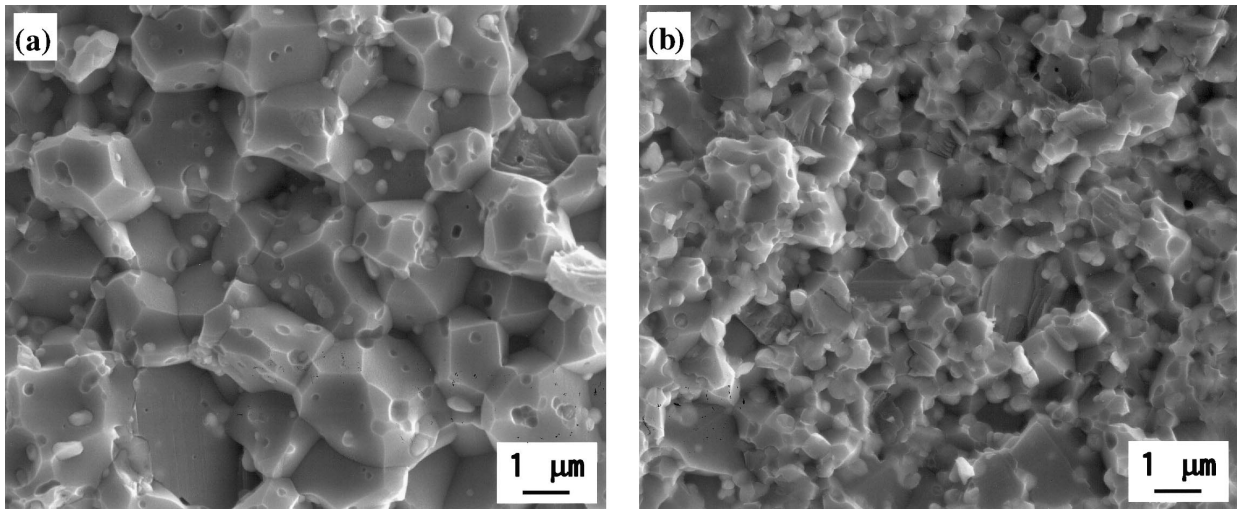

Fig. 3. SEM photographs for the fracture surfaces of the MgO/5 (a) and 20 vol% $BaTiO_3$ nanocomposites (b) PECSed at 1300°C for 10 min.

and electric field effect appears to be responsible for such an excellent sinterability in the MgO/$BaTiO_3$ nanocomposites prepared by the PECS.[13]

An addition of $BaTiO_3$ particle results in the significant increase of the relative density of the MgO, in particular, in the MgO/$BaTiO_3$ nanocomposites sintered at 1200°C by PECS technique. Although the relative density of the monolithic MgO was less than 80%, it increased as a function of $BaTiO_3$ content. The relative density showed a maximum value with an addition of 40 vol% of $BaTiO_3$, and thereafter it slightly decreased with $BaTiO_3$ content. This observed sintering behavior indicates that the $BaTiO_3$ particles can accelerate the sinterability of the MgO ceramics. The density reduction in the MgO/60, 80 vol% $BaTiO_3$ nanocomposites and $BaTiO_3$ might be caused by incorporation of pores into the matrix grains due to the extremely high heating rate of the PECS technique.

Figure 5 shows the high angle ($2\theta = 91$–$93°$) X-ray diffraction profiles of the MgO/10 vol% $BaTiO_3$ nanocomposite sintered at 1200°C by PECS in order to investigate the crystal structure of the $BaTiO_3$ dispersoids. It is known that the groups of reflection planes of (213), (312) and (321) are very sensitive to the crystal structure variation of $BaTiO_3$. The cubic structure gives a set of doublets formed by reflections from the same phase of the two wave length $K\alpha_1$ and $K\alpha_2$. Whereas, in the tetragonal structure each doublet is split into a set of partly overlapping doublets.[14] A diffraction profile (a) is one of the starting MgO/10 vol% $BaTiO_3$ powder; it has four well-defined split peaks which originate from the tetragonal structure of $BaTiO_3$. On the other hand, the profile of the as-PECSed MgO/10 vol% $BaTiO_3$ nanocomposite [Fig. 5(b)] indicated that the $BaTiO_3$ dispersoids are not tetragonal but cubic structure. Although

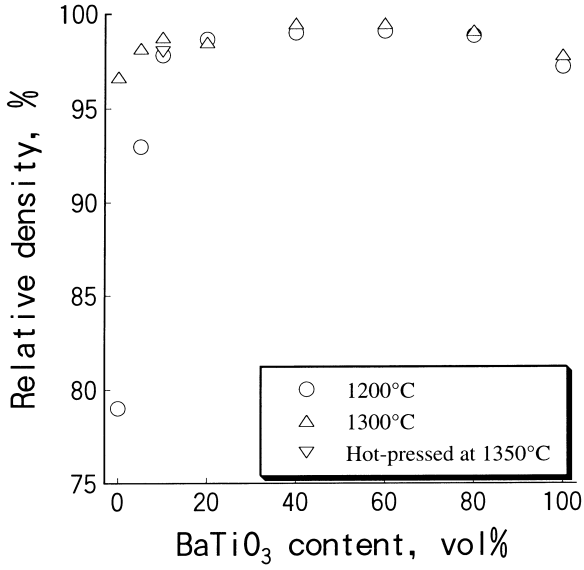

Fig. 4. Relative density of the monolithic MgO and MgO/$BaTiO_3$ nanocomposites as a function of $BaTiO_3$ content.

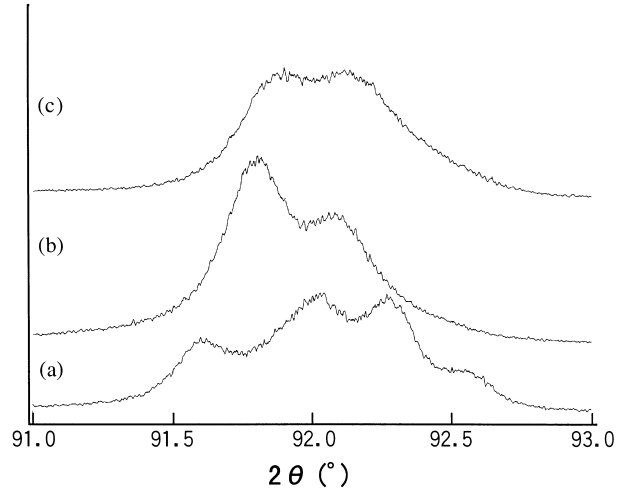

Fig. 5. High angle ($2\theta = 91$–$93°$) X-ray diffraction profiles of the starting MgO/5 vol% $BaTiO_3$ powder (a) MgO/10 vol% $BaTiO_3$ nanocomposite sintered at 1200°C for 10 min (b) and MgO/10 vol% $BaTiO_3$ nanocomposite sintered at 1200°C and annealed at 1200°C for 1 h (c).

the diffraction profile of the nanocomposite PECSed at 1200°C for 10 min and subsequently annealed at 1200°C for 1 h [Fig. 5(c)] was not the typical tetragonal peaks mentioned above, the shoulder of the diffraction peak on the lower angle side indicated the tetragonal distortion of the $BaTiO_3$ dispersoids. These results are similar to our previous work[10] and are considered to be associated with the incorporation of Mg^{2+} ions into the perovskite structure or residual thermal stress due to the thermal expansion mismatch between the MgO matrix and $BaTiO_3$ dispersoids. The peaks of the $BaTiO_3$ dispersoids in the MgO/$BaTiO_3$ nanocomposites prepared by the PECS technique is better split than those of the hot-pressed nanocomposites. Therefore, it was found that the PECS is a good sintering technique to increase the tetragonality of the $BaTiO_3$ dispersoids.

4 Conclusions

MgO/$BaTiO_3$ nanocomposites were successfully fabricated by the PECS technique. $BaTiO_3$ was the phase compatible with the MgO matrix. The nanocomposites consisted of MgO and tetragonal $BaTiO_3$. $BaTiO_3$ particles were homogeneously dispersed in the MgO matrix. The average size of the $BaTiO_3$ particles increased with $BaTiO_3$ content and the ratio of intergranular to intragranular $BaTiO_3$ particles also increased. The PECS technique had a remarkable effect on accelerating the sinterability of the MgO matrix. It was found that fully densified MgO/10 vol% $BaTiO_3$ nanocomposite could be fabricated when sintering the nanocomposite at 1200°C for 10 min. It seems that the $BaTiO_3$ particles also enable us to improve the sinterability of the MgO matrix. The $BaTiO_3$ dispersoids in the nanocomposite prepared by the PECS technique showed better defined tetragonal distortion than that of the hot-pressed nanocomposite and it meant that the PECS technique was effective to increase the ferroelectricity of the MgO/$BaTiO_3$ nanocomposites.

Acknowledgements

This work was has been carried out as part of the Synergy Ceramics Project under the Industrial Science and Technology Frontier (ISTF) Program promoted by AIST, MITI, Japan. Under this program, part of the work has been funded through NEDO. The authors are members of the Joint Research Consortium of Synergy Ceramics.

References

1. Niihara, K., Nakahira, A., Sasaki, G. and Hirabayashi, M., Development of strong Al_2O_3/SiC composites. In *Proceeding of the MRS International Meeting on Advanced Materials*, Tokyo, Japan. Plenum Press, Tokyo, Japan, 1988, pp. 129–134.
2. Niihara, K., New design concept of structural ceramics—ceramic nanocomposites. *J. Ceram. Soc. Jpn.*, 1990, **99**(10), 974–982.
3. Niihara, K. and Nakahira, A., Particle-strengthened oxide ceramics, nanocomposites. In *Advanced Structural Inorganic Composites*. ed P. Vincentini. Elsevier Science, Trieste, Italy, 1990, pp. 637–664.
4. Ohji, T., Nakahira, A., Hirano, T. and Niihara, K., Tensile creep behavior of alumina/silicon carbide nanocomposites. *J. Am. Ceram. Soc.*, 1994, **77**(12), 3259–3262.
5. Mizutani, T., Kusunose, T., Sando, M. and Niihara, K., Microstructure and properties of nano-sized BN-particulate-dispersed sialon ceramics. In *Proceeding of 6th Int'l Symp. Ceramic Materials and Components for Engines*, Arita, Japan, eds K. Niihara, S. Kanzaki, K. Komeya, S. Hirano and K. Morinaga. Techniplaza Co., Ltd., Tokyo, 1998, pp. 876–881.
6. Sekino, T., Nakajima, T., Ueda, S. and Niihara, K., Reduction and sintering of a nickel-dispersed-alumina-based nanocomposite and its properties. *J. Am. Ceram. Soc.*, 1997, **80**(51), 1139–1148.
7. Awano, M., Synthesis of ceramic nanocomposite with a magnetic sensing ability. *Bull. Ceram Soc. Jpn.*, 1997, **32**(12), 997–999 (in Japanese).
8. Noma, T., Wada, S., Sakake, M., Otsuka, T. and Suzuki, T., Indentation fracture of poled barium titanate ceramics. In *Proceedings of the Annual Meeting of the Ceramic Society of Japan*, Yokohama, Japan, April 1996. The Ceramic Society of Japan, Tokyo, Japan, 1996, p. 551 (in Japanese).
9. Okazaki, K., Mechanical behavior of ferroelectric ceramics. *Ceram. Ceram. Soc. Bull.*, 1984, **63**(91), 1150–1152.
10. Nagai, T., Hwang, H. J., Yasuoka, M., Sando, M. and Koichi Niihara, Preparation of a barium titanate-dispersed-magnesia nanocomposite. *J. Am. Ceram. Soc.*, 1998, **81**(21), 425–428.
11. Kondo, I., Tanaka, T. and Tamari, N., Usefulness of spark plasma sintering on densification and mechanical properties of alumina whisker/zirconia composites. *J. Ceram. Soc. Jpn.*, 1994, **102**(51), 505–507.
12. Tamari, N., Tanaka, T., Tanaka, K., Kondo, I., Kawahara, M. and Tokita, M., Effect of spark plasma sintering on densification and mechanical properties of silicon carbide. *J. Ceram. Soc. Jpn.*, 1994, **102**(51), 505–507.
13. Choa, Y. H., Kawasaki, H., Sekino, T. and Niihara, K., Microstructure and mechanical properties of oxide based nanocomposites fabricated by spark plasma sintering. *Key Eng. Mat.*, 1997, **132–136**, 2009–2012.
14. Hanafi, Z. M., Ismail, F. M., Hammad, F. F. and Nasser, S. A., Structural investigation of the phase transition in perovskite titanate containing additives. *J. Mat. Sci.*, 1992, **27**, 3988–3992.